Phytoplankton biomass and community composition in three Texas estuaries differing in freshwater inflow regime

Tiffany Chin [1,2]
Tiffany.Chin@uvm.edu
[1] Affiliation at time of research, [2] Current address

Laura Beecraft [1*]
Laura.beecraft@tamucc.edu
ORCID: ORCID: 0000-0001-5668-6687

Michael Wetz [1]
Michael.Wetz@tamucc.edu

[1] Harte Research Institute for Gulf of Mexico Studies
6300 Ocean Drive, Unit 5869 Corpus Christi, Texas 78412
[2] Rubenstein School of Environment and Natural Resources, University of Vermont, Burlington, Vermont 05405
*corresponding author

Running head: Inflow effects on phytoplankton communities

Keywords: Chlorophyll; Estuary; Salinity; Nutrients; Diatoms; *Aureoumbra lagunensis*

Regional terms: USA, Texas, San Antonio Bay, Nueces-Corpus Christi Bay, Baffin Bay

Abstract

Because many estuaries worldwide are experiencing large-scale alterations in freshwater inflows due to climatic and human influences on watersheds, it is critical to understand ecosystem-level responses to freshwater inflow conditions and variability. This study compared environmental conditions and phytoplankton biomass/community composition among three Texas estuaries with differing freshwater inflow regimes to understand the impacts of freshwater inflow magnitude on phytoplankton communities. It was hypothesized that: 1) nutrient concentrations and phytoplankton biomass would be highest in San Antonio Bay (SA), the high inflow estuary and lower in Nueces-Corpus Christi Bay (NC) and Baffin Bay (BB) due to lower average inflows, and 2) the phytoplankton community would be dominated by large and/or fast-growing taxa in SA, with a greater fraction of small and/or slow-growing taxa in NC and BB. Highest inorganic nutrient concentrations were generally observed in SA, while high organic nutrient concentrations were found in BB. Chlorophyll *a* was relatively high in both SA and BB (mean 16.9-18.5 $\mu g\ L^{-1}$) while phytoplankton biovolume was highest in BB. Despite distinct freshwater inflow, salinity and nutrient regimes, differences in phytoplankton community composition were less pronounced. Nano- or microplankton were the dominant size class of phytoplankton in each system, and diatoms were the dominant functional group, accounting for 27-49% of total biovolume on average. There were indications that the phytoplankton community was more diverse in SA, especially following inflow events, providing evidence that inflow may act as a disturbance that leads to greater phytoplankton diversity. Results from this study also showed that while freshwater inflow is important for nutrient delivery, low inflow estuaries such as BB are still susceptible to effects of eutrophication due to long residence times and nutrient retention/recycling. Overall, the differing responses of each of these ecosystems to

freshwater inflow highlight the importance of system-specific management plans and consistent monitoring programs in coastal estuaries.

Abbreviations

BB – Baffin Bay; DIN – dissolved inorganic nitrogen; DNRA - dissimilatory nitrate reduction; DO – dissolved oxygen; DOC – dissolved organic carbon; DON – dissolved organic nitrogen; HAB – harmful algal bloom; N – nitrogen; NC – Nueces-Corpus Christi Bay, SA – San Antonio Bay; TDN – total dissolved nitrogen; TOC – total organic carbon

Introduction

Freshwater inflows bring new nutrients and sediment loads to estuaries, affecting biogeochemical processes (Sklar and Browder 1998; Bruesewitz et al. 2013), light availability in the water column (Underwood and Kromkamp 1999; Azevedo et al. 2014), and primary production (Lancelot and Muylaert 2011). Additionally, the magnitude of freshwater entering an estuary influences mixing, circulation patterns, and hydraulic flushing regimes (Longley 1994; Montagna et al. 2018). Freshwater inflows are variable at the scale of individual bays and are dependent on both short-term weather patterns and long-term climatic variation, as well as human influences such as damming and freshwater withdrawals (Kennish 2002; Montagna et al. 2013).

Phytoplankton are sensitive indicators of environmental change because of their ability to respond rapidly to acute or chronic perturbations (Paerl et al. 2007; Lemley et al. 2016). This, as well as their position at the base of the estuarine food web, highlights the importance of understanding phytoplankton responses to large-scale environmental drivers such as freshwater

inflow variability. Freshwater inflow influences estuarine phytoplankton through multiple interacting factors, primarily nutrient regime and flushing time. Nutrient inputs often scale to the level of freshwater inflow and can stimulate phytoplankton growth (Mallin et al. 1993), but high magnitude inflows may limit biomass accumulation when flushing times exceed phytoplankton growth rates (Roelke et al. 2013; Azevedo et al. 2014). Higher inflows may also increase sediment loading, which could result in decreased light availability in the water column, introducing the potential for light limitation (Lancelot and Muylaert 2011). Alternatively, estuarine phytoplankton growth can become nutrient limited under prolonged low-flow conditions in some estuaries such as North Carolina's (USA) Neuse River Estuary (e.g. Wetz et al. 2011), although other studies have shown that phytoplankton growth can continue by utilizing regenerated nutrients, especially in shallow lagoonal systems (Glibert et al. 2010). In addition to influencing phytoplankton growth, freshwater inflow variability can affect phytoplankton community composition. Under high inflow regimes, large and/or fast-growing taxa such as diatoms or chlorophytes are expected to dominate, as they can rapidly uptake (and even store) new nutrients (Paerl et al. 2014; Carstensen et al. 2015; Cloern 2017). Under low inflow regimes, low "new" nutrient concentrations and greater availability of recycled or organic nutrients may be advantageous for picocyanobacteria due to high surface area to volume ratios, and to mixotrophic dinoflagellates that are also advantaged by longer residence times due to their slower growth rates (Glibert et al. 2010; Longphuirt et al. 2019). There are exceptions, however. For example, blooms of some dinoflagellate taxa have been linked to high inflow and high nutrient conditions (e.g., Litaker et al. 2002; Carstensen et al. 2015).

Along the Texas coast, there is a precipitation gradient that results from a humid, subtropical climate in the north to an arid climate in the south (Texas Water Development Board

2019). This gradient results in diminishing freshwater inflows along the coast, shifting from river-dominated estuaries in the north to low-inflow hypersaline systems in the south (Montagna et al. 2018). Freshwater inflow to many Texas estuaries has been decreasing over the past century due to damming, drought, and water withdrawals (Montagna et al. 2013), while climate change projections suggest that precipitation (and subsequent inflows) will decrease further by the end of the 21st century along the central and south Texas coast (Nielsen-Gammon et al. 2020). Increasing freshwater demands from population growth in coastal areas are likely to exacerbate the effects of this freshwater inflow reduction (Montagna et al. 2013). These changes could impose stress on estuarine ecosystems by starving estuarine primary producers of limiting nutrients, and thereby negatively affecting food available to higher trophic levels (e.g., Nixon 2003). This oligotrophication has also been shown to cause a shift in phytoplankton community composition favoring harmful algal bloom (HAB) species in other estuaries (Collos et al. 2009). In Texas, resource managers need to understand the relationship between freshwater inflows and ecosystem structure and function to fulfill state regulatory requirements. Aside from this localized need, the natural inflow gradient that is present on the Texas coast affords an opportunity to quantify large-scale relationships between freshwater inflow and phytoplankton biomass/community composition, and by comparing estuaries varying in inflows, may also offer a glimpse into the future condition of estuaries that are currently experiencing declining inflows.

Here we compared environmental and phytoplankton indicators among three estuaries differing in freshwater inflow regime: San Antonio Bay (SA), which is river-influenced, Nueces-Corpus Christi Bay (NC), considered a neutral estuary based on inflow balance, and Baffin Bay (BB), which has no major river inflows and is frequently hypersaline. Our objectives were to assess if the different freshwater inflow regimes led to differences in environmental conditions

and phytoplankton communities among the three bays, and if so, how. We hypothesized that 1) nutrient concentrations and phytoplankton biomass would be highest in the high inflow estuary (SA) and lower in NC and BB due to lower average inflows, and 2) the phytoplankton community would be distinct among bays and freshwater inflow conditions, dominated by large and/or fast-growing taxa in SA due to higher nutrient availability and flushing, with the fraction of small and/or slow-growing taxa increasing from NC to BB due to hypothesized lower nutrient concentrations and less flushing.

Methods

Site characteristics

Each of the estuaries examined in this study can be considered lagoonal systems that are separated from the adjacent Gulf of Mexico by barrier islands, limiting tidal influence and exchange of water (Fig 1). The diurnal tidal signature for each bay is generally <20-30 cm. SA is the northernmost of the three estuaries and is fed by the San Antonio and Guadalupe rivers. It receives the highest rates of freshwater inflow of the three estuaries and has a positive inflow balance (Montagna et al. 2018). The average depth of SA is 2 m (USEPA 1999), and the average residence time is 38 days (Montagna et al. 2011). The nearest inlet to the Gulf of Mexico is Pass Cavallo, located approximately 30 km to the north of the mouth of SA. The SA watershed is dominated by agricultural lands and scrub (NOAA C-CAP, https://coast.noaa.gov/digitalcoast/tools/lca.html). NC receives freshwater inflow from the Nueces River, as well as return flows from wastewater facilities. Because of damming and reservoir construction on the Nueces River, freshwater inflow magnitude has decreased considerably over time and only has a limited influence on the estuary. At present, inflow

balance is often neutral or slightly negative due to high evaporation rates and the low inflow rates (Montagna et al. 2018). The average depth of NC is 3 m, but an ~14 m deep ship channel facilitates exchange with the adjacent Gulf of Mexico (USEPA 1999). The average residence time of NC is 356 days (Montagna et al. 2011). Land use in the watershed is dominated by agriculture and developed areas (NOAA C-CAP). BB is the southernmost of the three estuaries. It has an average depth of 2 m and a negative inflow balance on average, resulting in frequent hypersalinity in the upper reaches of the bay (Wetz et al. 2017). Inflows in BB are from ephemeral streams, and the bay often experiences little to no inflow, punctuated by high inflow during El Niño years. The nearest inlets to the Gulf of Mexico are Packery Channel (~41 km north of Baffin Bay) and Port Mansfield (~80 km south of Baffin Bay). Cira et al. (2021) estimated that residence times range from ~3 weeks during high rainfall periods to many years during droughts, with an average residence time of > 1 year. Land use coverage in the BB watershed is dominated by agriculture, scrub/shrub, and grassland (NOAA C-CAP), and nutrient inputs are from these sources as well as failing sewage treatment infrastructure (Wetz et al. 2017; unpubl. data).

Field sampling

Monthly sampling was conducted in each bay from March 2018 to July 2019, except for April 2019 when BB was not sampled due to inclement weather. Six sites in BB and four sites each in SA and NC (Fig 1) were selected to capture the gradient from river influence to ocean exchange. The two additional sites in BB were included because BB has three tributaries with distinct environmental conditions. At each site, surface water (0.1 m) was collected in brown HDPE bottles and stored (i) on ice for nutrient, carbon, and chlorophyll *a* (Chl *a*) analysis and (ii) at ambient water temperature for phytoplankton enumeration. Sites in each bay are shallow

and rarely stratified such that a near-surface sample is representative of the water column. Secchi depth and depth profiles (every 0.5 m) of dissolved oxygen (DO), pH, conductivity, salinity, and temperature were collected using a Professional Plus YSI multiparameter sonde (YSI, Yellow Springs, OH).

Daily inflow data were obtained from USGS river gauges (http://waterdata.usgs.gov): San Antonio River (#08188500) and Guadalupe River (#08176500) for SA, Nueces River (#08211000) for NC, and Los Olmos Creek (#08212400), San Fernando (#08211900), and Petronila Creek (#08212820) for BB. Inflow averages were calculated for the seven days preceding each sampling date. This timeframe was chosen based on best methods reported by Roelke et al. (2017).

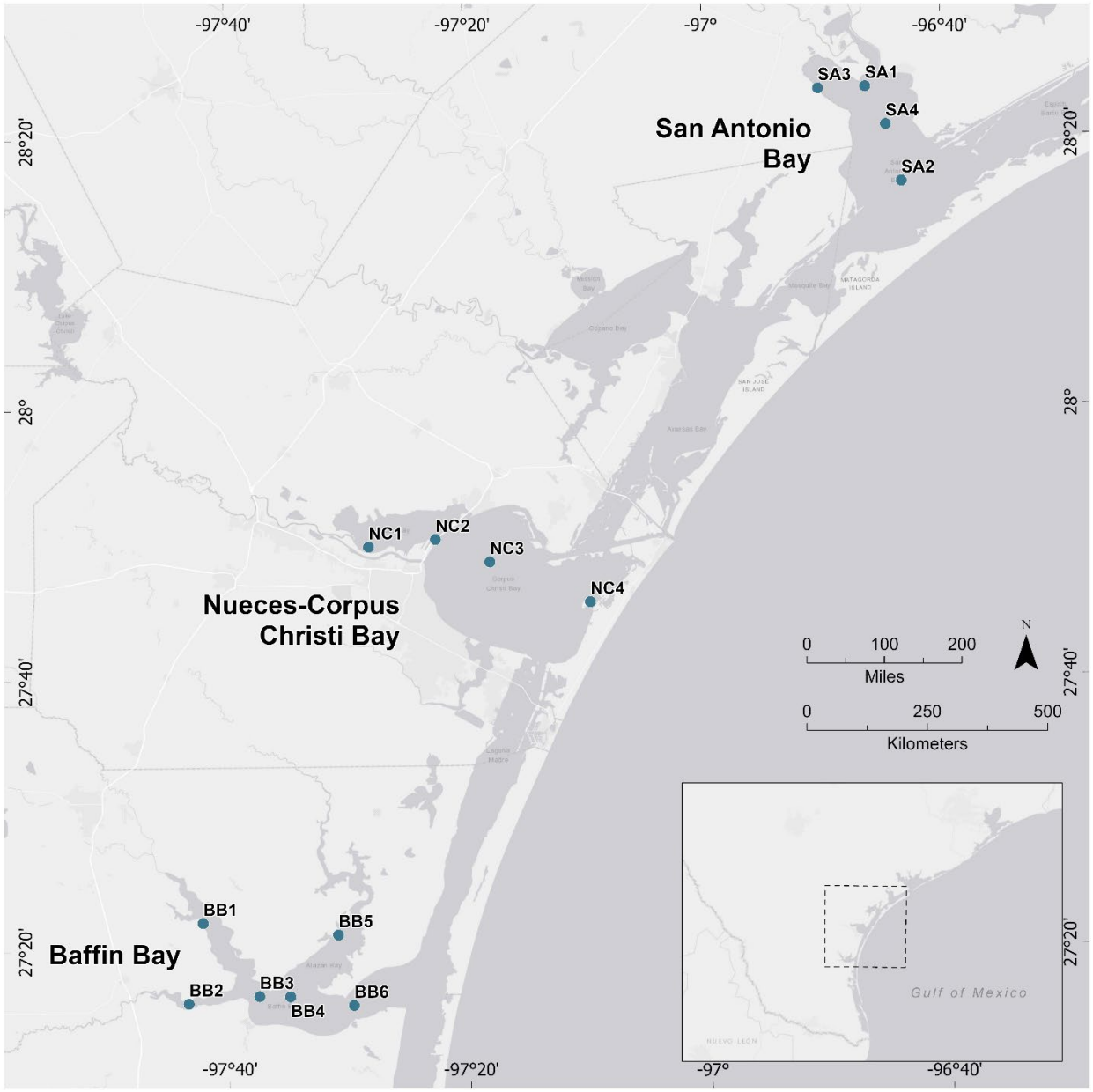

174

175 **Fig 1 Map of sampling sites within the 3 bays located along the Texas coast of the Gulf of**

176 **Mexico: Baffin Bay (6 sites), Nueces-Corpus Christi Bay (4 sites), and San Antonio Bay (4**

177 **sites).**

Water chemistry analyses

Inorganic nutrient (nitrate + nitrite (NO_x), ammonium, orthophosphate, and silicate) and total dissolved nitrogen (TDN) concentrations were determined from the filtrate of water samples that were passed through pre-combusted 25 mm GF/F filters and stored frozen (-20°C) until analysis. After thawing to room temperature, inorganic nutrient samples were analyzed on a Seal QuAAtro autoanalyzer. TDN samples were analyzed using the High Temperature Catalytic Oxidation method on a Shimadzu TOC-Vs analyzer with nitrogen module. Dissolved organic nitrogen (DON) was determined by subtracting dissolved inorganic nitrogen (DIN; ammonium, NO_x) from TDN. Full details on analytical methods can be found in Wetz et al. (2017).

Phytoplankton quantification

Chl *a* was analyzed for total, <20 µm, and <3 µm size fractions. The <20 and <3 µm size fractions were pre-filtered through 20 µm mesh or Whatman GF/D filters (nominal pore size 2.7 µm, referred to here as 3 µm), respectively. Samples were collected on 25 mm Whatman GF/F filters at low vacuum pressure (<5 mm Hg) and stored frozen (-20°C) until analysis. Chl *a* was quantified fluorometrically following passive extraction in 90% acetone for 16-24 h, without acidification, using a Turner Trilogy fluorometer (Welschmeyer 1994).

Phytoplankton were quantified using a combination of flow cytometry (picophytoplankton and *Aureoumbra lagunensis*) and microscopic identification. Samples for flow cytometric analysis were fixed with glutaraldehyde (ca. 0.002%) and stored at -20°C until analysis. Samples were thawed in the dark at room temperature, filtered through 20 µm Nytex mesh, and processed on an Accuri C6 Plus flow cytometer (BD BioSciences, San Jose CA) for picophytoplankton quantification (Marie et al. 1999). Additionally, samples for *A. lagunensis* enumeration were stained using a species-specific polyclonal antibody and run in parallel with

unstained controls. The detection limit for *A. lagunensis* enumeration was 80,000 cells·ml^{-1} (Cira and Wetz 2019), and values below detection limit were treated as zeros. *A. lagunensis* has been known to form persistent, near mono-specific blooms in BB since 1990 (Wetz et al. 2017; Cira and Wetz 2019), and hence special attention was paid to it.

Nano- and microplankton were enumerated using the Utermöhl method with samples preserved with acid Lugol's (ca. 2%). Samples (5-10 mL) were settled for 24 hours and counted using an Olympus 1X-71 inverted microscope at 200x magnification. Biovolume was estimated from formulas of geometric shape of cells as described by Hillebrand et al. (1999) and Sun and Liu (2003). When there were conflicts between the formulas in these two sources, formulas from Sun and Liu (2003) were used. Taxa were grouped into nine categories: diatoms, dinoflagellates, euglenoids, unidentified flagellates, cyanobacteria, chlorophytes, *Mesodinium, A. lagunensis*, and other unidentified taxa. *Mesodinium* (syn. *Myrionecta*) is included because it is a distinctive mixotrophic ciliate containing chloroplasts and contributes to observed Chl *a* concentrations.

Statistical Analyses

A ln(x+1) transformation was applied prior to some analysis to improve normality, except for relative contributions (i.e. percentages) of phytoplankton size classes and groups. Statistical analyses were performed using PC-ORD Version 7.08 (McCune & Mefford, 2018) and R version 4.1.0 (R Core Team 2020), including tidyverse (Wickham et al. 2019), skimr (Waring et al., 2021), rstatix (Kassambara 2020) and broom (Robinson and Hayes 2020) packages.

Regression analyses and property-property plot visualization of salinity compared to select nutrient and phytoplankton parameters were used to assess the effect of inflow. One-way

223 analysis of variance (ANOVA) and Tukey's HSD was used to assess differences in individual
224 environmental and phytoplankton variables among bays.

225 Principal Components Analysis (PCA) of the correlation cross-products matrix was used
226 to visualize patterns of environmental responses among bays, and Non-metric Multidimensional
227 Scaling (NMS) analysis using the Bray-Curtis distance matrix was used to visualize patterns in
228 community composition based on phytoplankton group biovolume. Single factor permutation-
229 based significance tests (multiple-response permutation procedures, MRPP) was also used to
230 compare environmental (Euclidean distance matrix) and biovolume composition (Bray Curtis
231 distance matrix) responses among bays.

232 ## Results

233 ### Comparison among bays

234 The anticipated gradient of freshwater inflow among bays was observed, with average
235 freshwater inflows of 76.4 $m^3 s^{-1}$ to SA, 24.3 $m^3 s^{-1}$ to NC, and 0.2 $m^3 s^{-1}$ to BB (Fig 2, Table 1).
236 This corresponded to an inverse pattern in salinity, with average salinity of 10.1 in SA, 25.5 in
237 NC and 35.7 in BB (Fig 2, Table 1). The study encompassed a relatively dry period from March-
238 September 2018, when ~97% of the central Texas coastal region was in mild to moderate
239 drought conditions (unpubl. data obtained from U.S. Drought Monitor). Thereafter, wet
240 conditions generally persisted.

241 Multivariate analyses indicated that environmental and water chemistry parameters were
242 distinct among the three bays (MRPP: test statistic = -92.66, p-value < 0.001, Association =
243 0.305), visualized by spatial separation among bays in the PCA ordination (Fig 3). The first and
244 second axes of the PCA ordination cumulatively explain 55% of the observed variation in the

cross products matrix of transformed environmental response data (31.8 and 23.2%, respectively). SA samples were positively associated with freshwater inflow (average 7-day inflow prior to sampling dates) and inorganic nutrients, in particular NO_x and orthophosphate, BB samples were associated with higher salinity and often with increased DON, while NC samples were intermediate between SA and BB with respect to the inflow-salinity gradient.

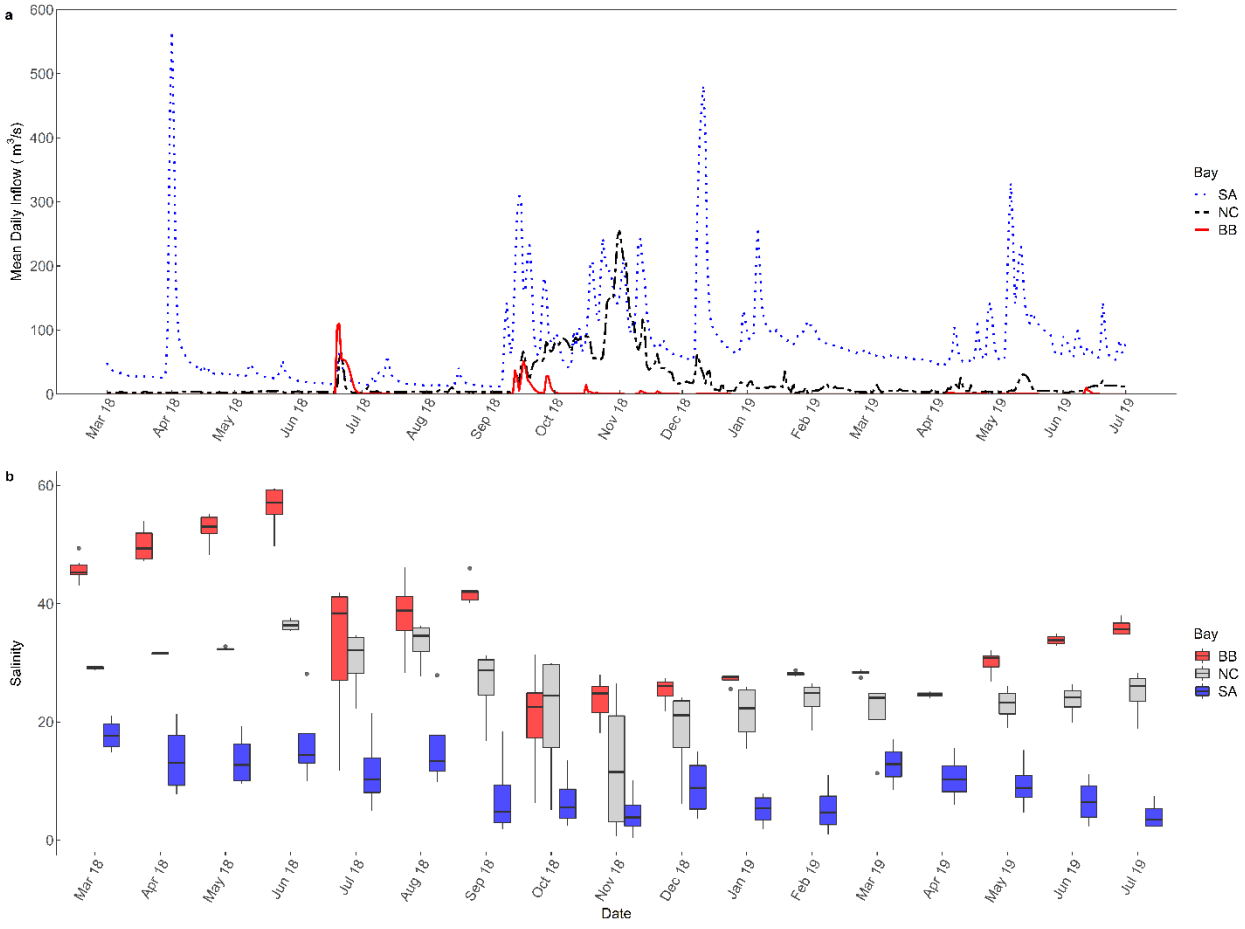

Fig 2 Mean daily inflow (a) calculated from USGS daily river gauge data and boxplots of salinity (b) measured monthly at multiple sites within each bay, color coded by bay.

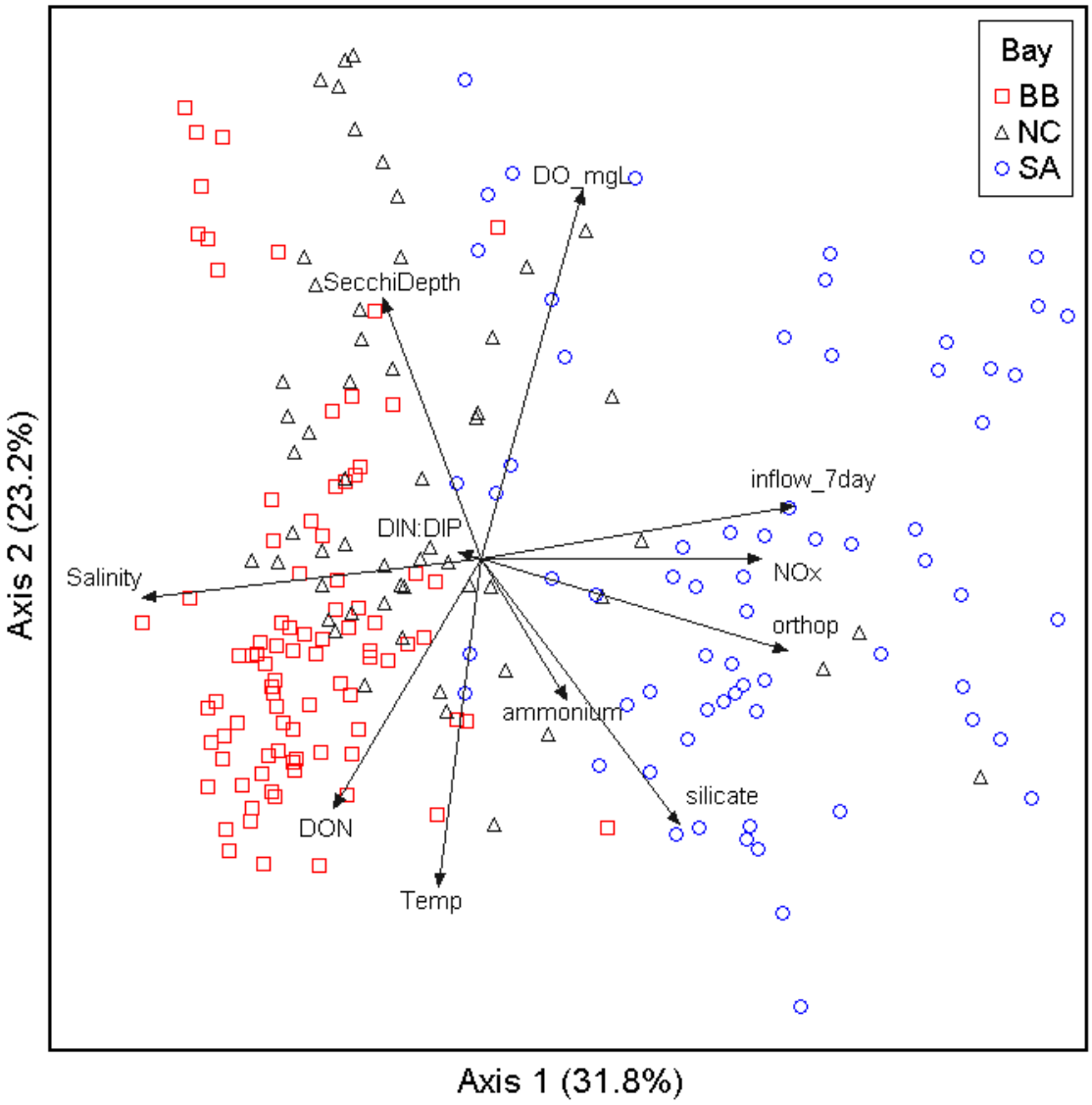

Fig 3 Principal Components Analysis (PCA) of select environmental and water chemistry response parameters measured at multiple sites in San Antonio (SA), Nueces-Corpus Christi (NC), and Baffin (BB) Bays over the 17-month sample period.

Table 1 Summary of environmental and phytoplankton community variables in Baffin Bay, Nueces-Corpus Christi Bay and San Antonio Bay. Values are mean and range measured across all sampling dates and sites within each bay. Superscript letters indicate significant differences between bays based on 1-way ANOVA and Tukey's HSD pairwise comparisons. Refer to Supplementary Materials for complete ANOVA results (Table S1). ANOVA comparisons for relative group contribution to total biovolume were performed for groups with at least 50% of observations > 0 for each site.

	Baffin Bay		Nueces-Corpus Christi Bay		San Antonio Bay	
	Mean	Min - Max	Mean	Min - Max	Mean	Min - Max
Inflow (7 d avg) ($m^3 \cdot s^{-1}$)	[a] 0.2	0 – 1	[b] 24.3	2.5 – 185.7	[c] 76.4	18.4 – 223.6
Salinity	[a] 35.7	6.3 – 59.5	[b] 25.5	0.7 – 37.6	[c] 10.1	0.3 – 28.1
Secchi Depth (m)	[a] 0.5	0.2 – 1.2	[b] 0.7	0.2 – 2.2	[c] 0.4	0.1 – 1.2
Ammonium (µM)	[a] 3.7	0 – 15.9	[b] 1	0 – 11.2	[a] 4.3	0.2 – 25.8
NOx (µM)	[a] 1.5	0.1 – 18.1	[b] 0.6	0.1 – 5.5	[c] 22.2	0.1 – 118.8
Orthophosphate (µM)	[a] 0.8	0 – 8.2	[b] 1.5	0 – 10.6	[c] 3.2	0.1 – 8.9
Silicate (µM)	[a] 100.6	4.5 – 280	[a] 103.9	9.5 – 462.9	[b] 149.5	26.6 – 301.3
DON (µM)	[a] 69.1	45.9 – 111.2	[b] 35.3	17.9 – 64.5	[b] 38.6	10.1 – 78.3
DIN:DIP	[a] 41.5	0.1 – 886.3	[b] 2.7	0 – 29.3	[a] 12.1	0.2 – 108.6
Total Chlorophyll a ($\mu g \cdot L^{-1}$)	[a] 18.6	3.6 – 62.8	[b] 9.6	4 – 17.3	[a] 17.2	2 – 59.2
Percent microplankton Chl *a*	[a] 29.5	0.9 – 87.9	[ab] 24.2	2.6 – 81.6	[b] 17.9	0.1 – 74.5
Percent nanoplankton Chl *a*	[a] 61.7	11.5 – 90	[ab] 67.2	14.2 – 91	[b] 72.4	22.6 – 94.7
Percent picoplankton Chl *a*	[a] 8.8	0.3 – 26.4	[a] 8.6	0.7 – 54	[a] 9.8	0.4 – 39.7
Total Biovolume ($\mu m^3 \cdot mL^{-1}$)	[a] $1.24 \cdot 10^7$	$(1.63 \cdot 10^5) – (7.78 \cdot 10^8)$	[b] $8.81 \cdot 10^5$	$(1.67 \cdot 10^5) – (4.86 \cdot 10^7)$	[b] $1.02 \cdot 10^6$	$(3.56 \cdot 10^4) – (6.81 \cdot 10^6)$
Percent diatoms	[a] 42.8	0 – 100	[a] 49.4	0 – 99.1	[b] 26.7	0 – 93.6
Percent dinoflagellates	[a] 16.5	0 – 91.8	[ab] 22.8	0 – 91.2	[b] 24.8	0 – 94.8
Percent picocyanobacteria	[a] 26.4	0 – 86.9	[b] 15.9	0.1 – 83.3	[ab] 19.6	0 – 85.6
Percent flagellates	[a] 4.8	0 – 87.3	[a] 5.7	0 – 62	[b] 13.1	0 – 73.6
Percent euglenophytes	3	0 – 99.9	0.7	0 – 14.3	1.8	0 – 25.2
Percent *Mesodinium*	1.6	0 – 65.6	1.1	0 – 11	7.4	0 – 94
Percent *A. lagunensis*	4	0 – 85.1	0	0 – 0	0	0 – 0
Percent chlorophytes	0	0 – 1.9	0	0 – 0.2	0.5	0 – 15.1
Percent unidentified	0.9	0 – 17.1	4.5	0 – 70.3	6.1	0 – 76.4

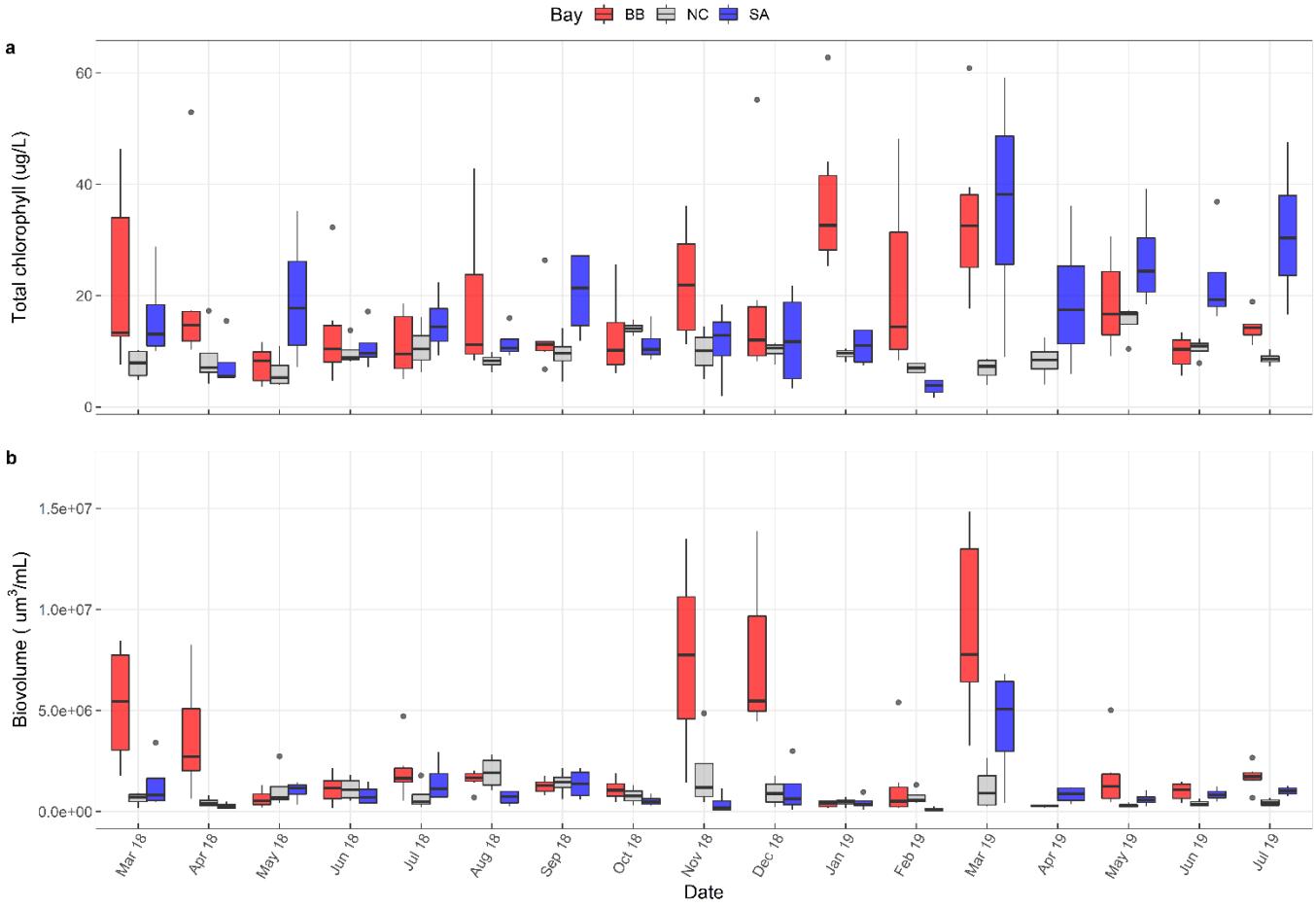

Fig 4 Total Chl *a* (a) and biovolume (b) over time, color-coded by bay. Note: an outlier point in December 2018 for site BB4 had a total biovolume of $7.78 \cdot 10^8$ µm^3 · mL is not shown within the y-range of this figure.

When examined individually, all environmental and water chemistry parameters except water temperature were significantly different among bays (ANOVA, $\alpha = 0.05$) (Table 1, Table S1). Secchi depth was shallowest in SA (mean = 0.4 m), intermediate in BB (0.5 m), and deepest in NC (0.7 m; Table 1). DON concentrations were much higher in BB (mean = 69.1 µM) compared to NC (35.3 µM) and SA (38.6 µM). NO_x concentrations were highest in SA (mean =

22.2 µM), intermediate in BB (1.5 µM), and lowest in NC (0.6 µM), while ammonium concentrations were higher in BB (3.7 µM) and SA (4.3 µM) compared to NC (1.0 µM). Orthophosphate concentrations were highest in SA (3.2 µM), intermediate in NC (1.5 µM) and lowest in BB (0.8 µM), while silicate concentrations were higher in SA (149.5 µM) compared to NC (103.9 µM) and BB (100.6 µM; Table 1).

Total Chl *a* was lower in NC compared to BB and SA (Table 1, Fig 4). The nanoplankton size class (3-20 µm) comprised most of the Chl *a* measured in all three systems, averaging 2-3 times higher concentrations compared to micro (>20 µm) and picoplankton (<3 µm) Chl *a* (Table 1). In BB, microplankton had higher relative contribution to total Chl *a* than in SA (Table 1), while the contribution of nanoplankton was lower in BB than SA. The micro- and nanoplankton size classes were not different between NC and the other two bays. The contribution of picoplankton was similar among all three bays (Table 1). Community composition based on group biovolume was statistically different among bays (MRPP: test statistic = -10.36, p-value < 0.001, association = 0.027). However, the within-group association was very low, indicating heterogeneity within the bays, consistent with the lack of visual separation of samples grouped by bay in the NMS ordination of biovolume community composition (Fig. S1). Total phytoplankton biovolume was significantly higher in BB compared to NC and SA (Table 1, Fig. 4). The ratio of Chl *a*:biovolume was higher for SA compared to NC and BB (Fig S2).

SA exhibited a relatively heterogeneous phytoplankton community on average, with contributions from diatoms (26.7% of total biovolume), dinoflagellates (24.8%), picocyanobacteria (19.6%) and unidentified flagellates (13.1%) (Table 1). In contrast, the contribution of diatoms was significantly higher in BB (42.8%) and NC (49.4%) than in SA. The contribution of dinoflagellates was highest in SA and NC (22.8%), and lower in BB (16.5%).

299 The contribution of picocyanobacteria was highest in BB (26.4%), lowest in NC (15.9%) and
300 intermediate in SA (19.6%). No other groups contributed ≥10% to total biovolume on average in
301 any of the bays.

302 ## Influence of inflow events

303 Silicate and orthophosphate displayed significant inverse correlations with salinity across
304 the three systems (Table 2, Table S2, Fig S3), indicating increasing concentrations with inflow.
305 NO_x also correlated inversely with salinity, though not significantly for BB, and with a higher
306 magnitude in SA. Ammonium showed no apparent correlation with salinity. Salinity did not have
307 a strong influence on phytoplankton biomass – a significant inverse correlation was only
308 observed between total Chl *a* and salinity for NC. Interestingly, there was a significant positive
309 correlation between salinity and total biovolume in SA, suggesting a flushing effect of inflow
310 that limited biomass accumulation (Table 2).

311 During the study period, distinct freshwater inflow events and/or prolonged periods of
312 rainfall affected each estuary. Although the study was not specifically designed to test for the
313 ecosystem response to specific inflow events as noted by the relatively low sampling frequency
314 (monthly), some additional insight can be drawn through examination of these periods. For
315 example, changes in nutrient concentrations observed during the inflow events are broadly
316 reflective of the differences observed between bays. NO_x increased sharply from 15 ± 9 µM to
317 37 ± 21 µM in SA during a brief high rainfall, high inflow period in April 2018 and again from 7
318 ± 6 µM to 41 ± 33 µM during a prolonged high rainfall, high inflow period that occurred in
319 September 2018-February 2019 (Fig 2, Fig 5), while NO_x either did not vary or decreased during
320 inflow events in BB occurring in June and September 2018 and in NC from September-
321 November 2018. Orthophosphate and silicate concentrations were generally higher in SA during

322 the wet period, with both peaking in October 2018 at 6.6 ± 1.7 µM and 224 ± 38 µM respectively
323 (Fig 5). A similar pattern was observed in NC and BB during high inflow periods.
324 Chl *a* initially decreased in SA coinciding with an April 2018 inflow event (from 16.2 ±
325 8.6 µg L^{-1} to 7.9 ± 5 µg L^{-1}) and then subsequently increased to 19.5 ± 12.4 µg L^{-1} in May 2018
326 (Fig 2, Fig 4). During the late 2018-early 2019 wet period, Chl *a* was variable and averaged 12.1
327 ± 7.2 µg L^{-1}, but as in May 2018, it increased considerably to 36.1 ± 21.4 µg L^{-1} as inflow, and
328 presumably flushing, decreased. In August 2018 just prior to the start of the prolonged wet
329 period, the phytoplankton community in SA had >90% biovolume of diatoms or dinoflagellates.
330 During the wet period, the community became more diverse, with several groups contributing
331 ≥10% of biovolume, including diatoms (21%), dinoflagellates (25%), flagellates (21%),
332 picocyanobacteria (10%) and *Mesodinium* (16%) (Fig 6). As inflow subsided and salinity began
333 to increase, however, a diatom bloom was eventually observed in March 2019. In NC, the
334 response of Chl *a* to freshwater inflow was equivocal at best, with responses varying by time and
335 date. In June 2018 just prior to the start of the wet period, diatoms were the dominant functional
336 group in NC, representing 33-86% of total biovolume depending on site (Fig 7). There was also a
337 large contribution of unidentified phytoplankton at the upper estuary site, NC1. Sites in the lower
338 estuary had a nominal contribution from dinoflagellates (8-26%) and picocyanobacteria (11-
339 32%). During the freshwater inflow events of summer-fall 2018, diatom relative abundance
340 decreased, while there was increased representation from dinoflagellates and picocyanobacteria,
341 and occasionally euglenoids and flagellates. In BB, Chl *a* changed little in response to a June
342 2018 inflow event but increased noticeably as inflow decreased following an inflow event in
343 September 2018 (Fig 2, 4). After the June 2018 event, the community became less diverse as
344 fewer functional groups contributed to the overall biovolume, particularly dinoflagellates and

picocyanobacteria (Fig 8). After the September 2018 event, there was no obvious immediate shift in community composition, although by November 2018 when inflow had decreased and salinity was increasing again, diatoms accounted for >95% of biovolume at all but one station (Fig 8).

Table 2 Slope parameters of linear regression analysis of salinity vs. nutrient and phytoplankton parameters for all observations combined and each bay individually. Bolded values are statistically significant at α = 0.05. Please refer to Table S2 for full details.

	All bays	SA	NC	BB
Ammonium (μM)	-0.02	0.10	0.01	-0.04
NO_x (μM)	**-0.62**	**-2.18**	**-0.05**	-0.04
Orthophosphate (μM)	**-0.09**	**-0.19**	**-0.20**	**-0.04**
Silicate (μM)	**-2.30**	**-4.14**	**-9.33**	**-0.34**
Total Chlorophyll *a* ($\mu g \cdot L^{-1}$)	-0.05	-0.14	**-0.13**	-0.21
Total Biovolume ($\mu m^3 \cdot mL^{-1}$)	$6.41 \cdot 10^4$	$\mathbf{5.48 \cdot 10^4}$	$1.54 \cdot 10^4$	$-7.17 \cdot 10^5$

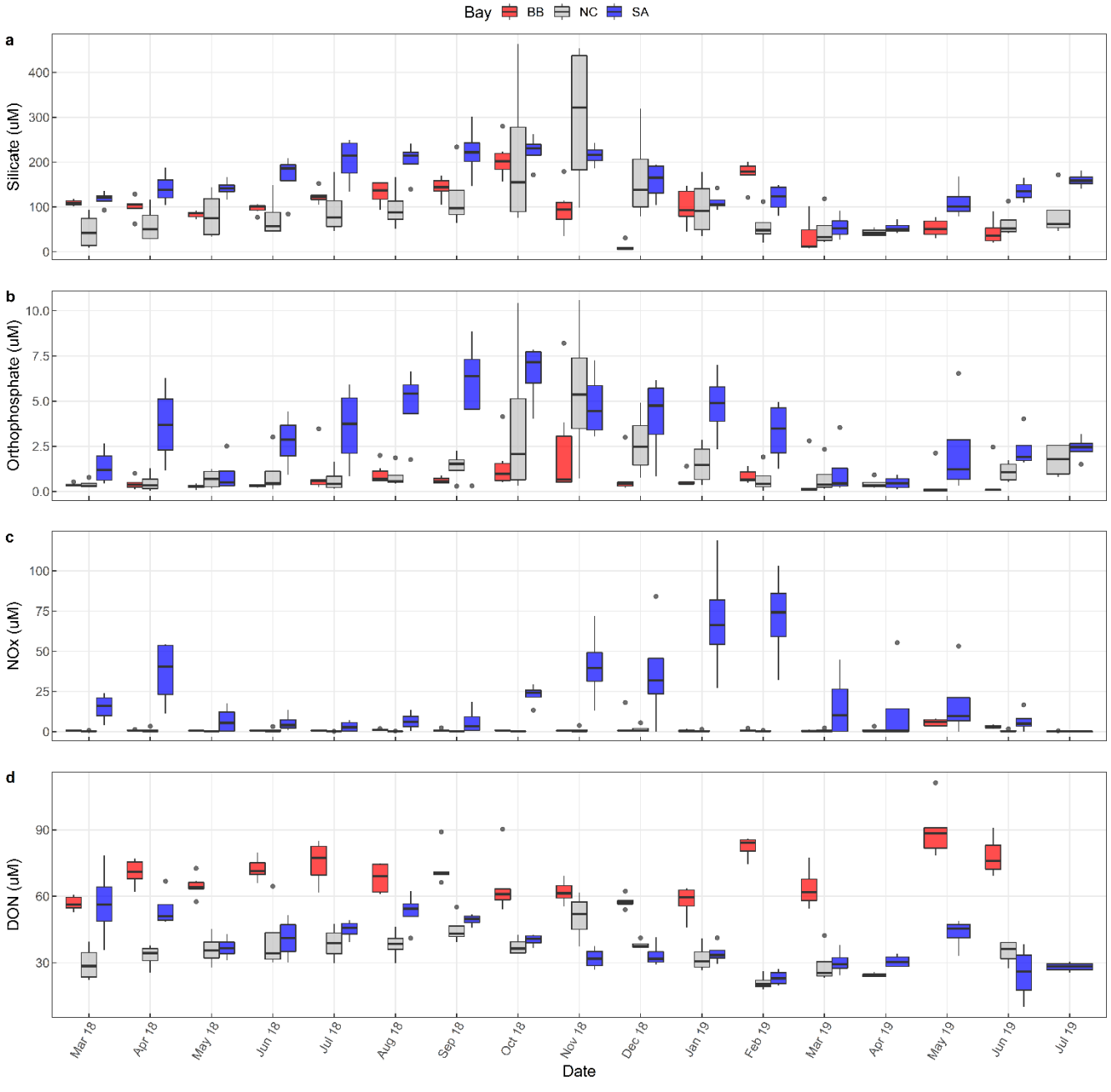

Figure 5 Boxplots of nutrient concentrations of (a) silicate, (b) orthophosphate, (c) NO_x and (d) DON summarized for all sampling sites on each sampling date over time, color-coded by bay.

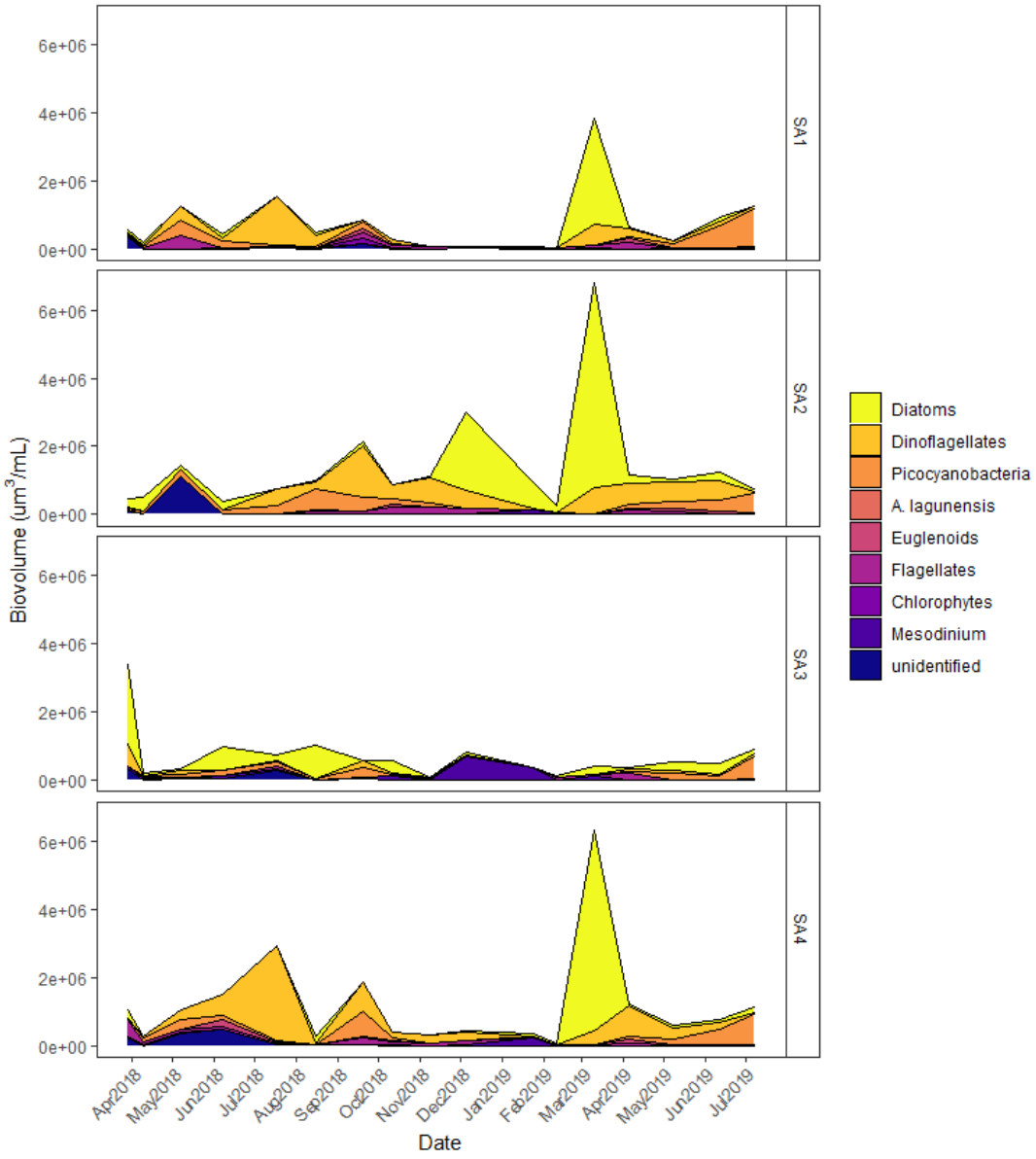

Fig 6 Phytoplankton biovolume color-coded by functional groups on each monthly sampling date, March 2018-July 2019, for each site (panels SA1 – SA4) in San Antonio Bay.

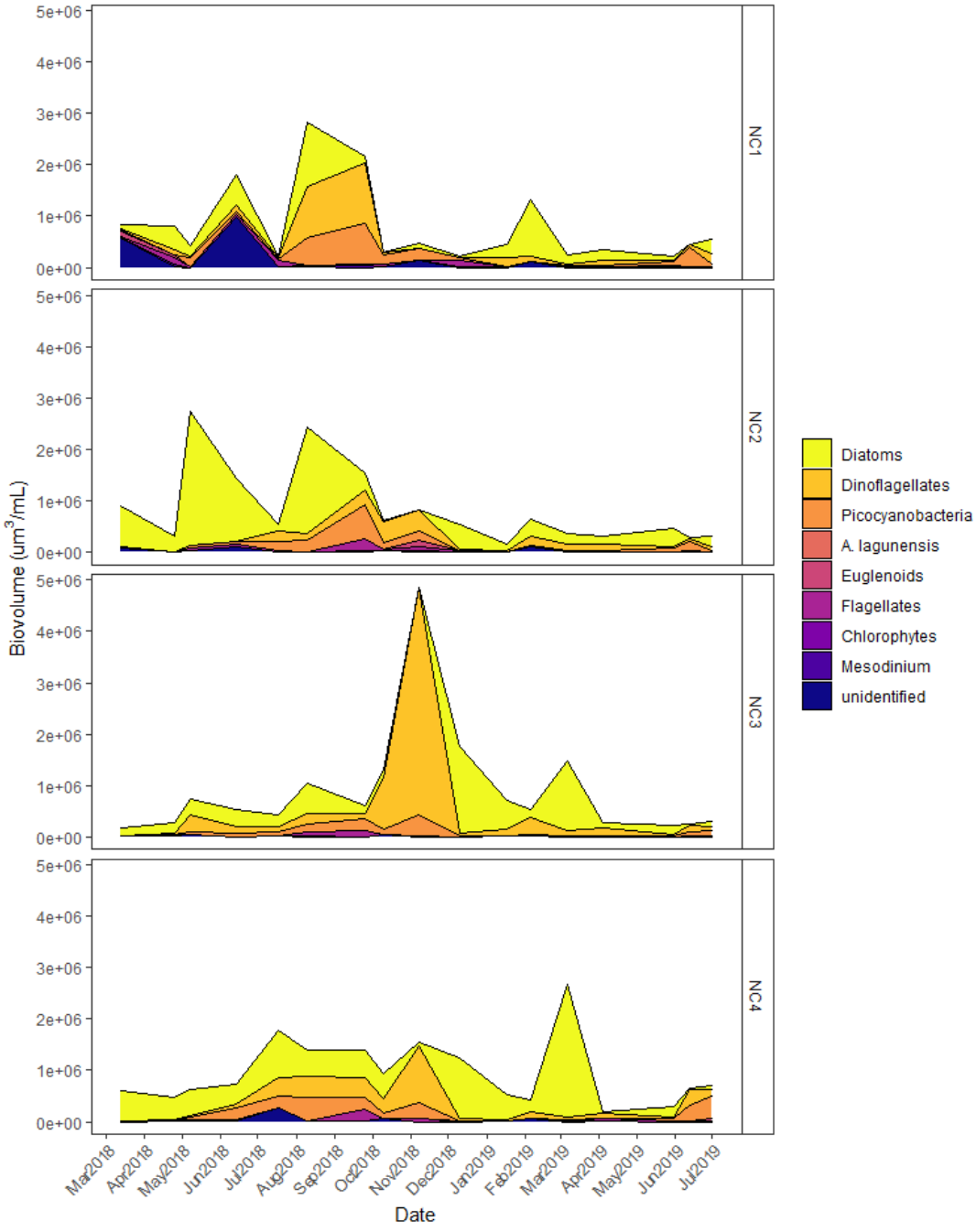

364

365 **Fig 7 Phytoplankton biovolume color-coded by functional groups on each monthly**

366 **sampling date, March 2018-July 2019, for each site (panels NC1 – NC4) in Nueces-Corpus**

367 **Christi Bay.**

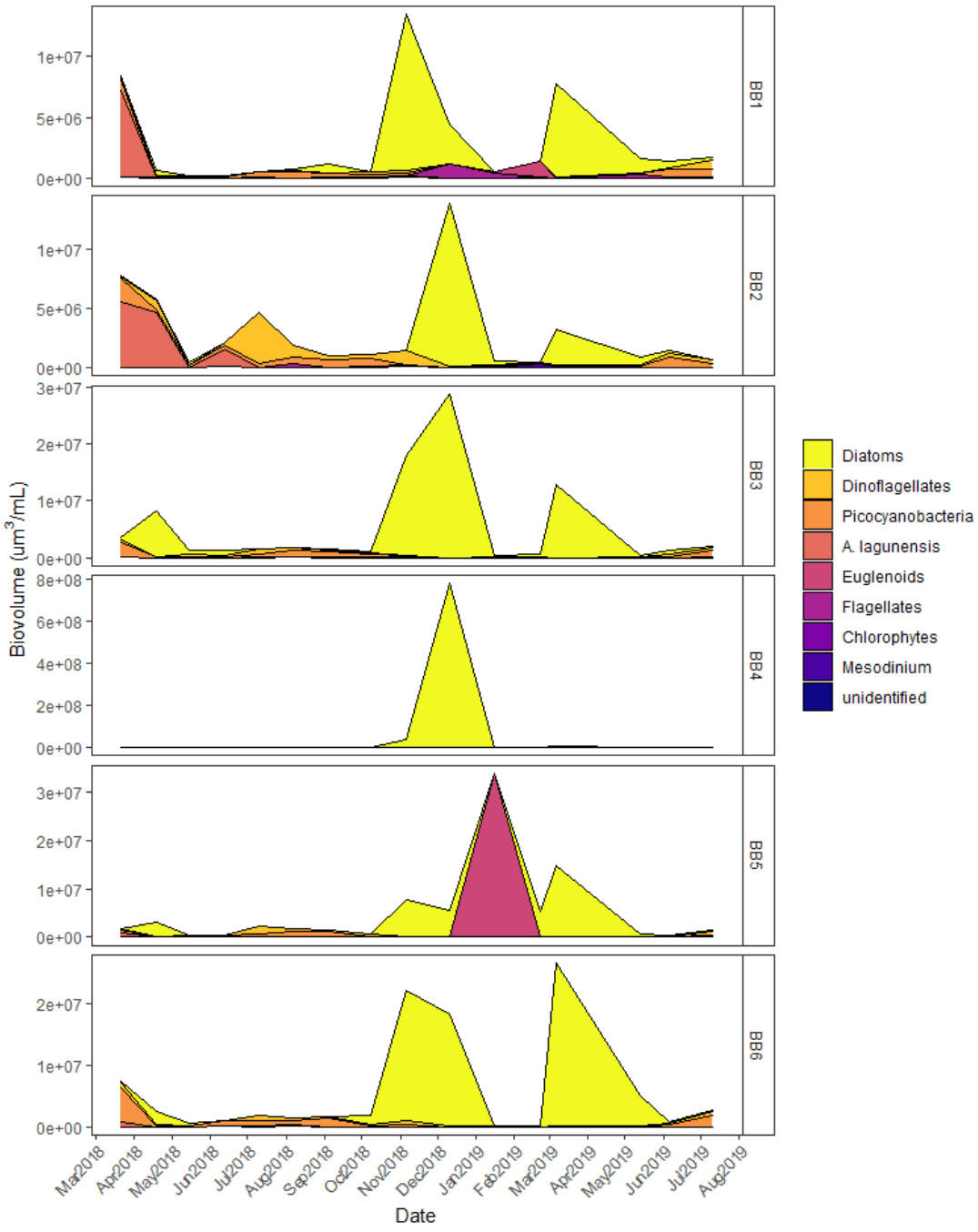

Fig 8 Phytoplankton biovolume color-coded by functional groups on each monthly sampling date, March 2018-July 2019, for each site (panels BB1 – BB6) in Baffin Bay. *Note: differences in y-axis scale among site panels, e.g. a large diatom bloom was

quantified at site BB4 in December 2018 that was an order of magnitude higher than any other sample, and presence of other groups is difficult to see.

Discussion

Freshwater inflow is an important driver of nutrient loading, flushing rates, and phytoplankton dynamics in estuaries, and in many coastal regions worldwide freshwater inflow rates are changing due to climatic and anthropogenic influences. Aside from freshwater inflow, there are other environmental factors that are also relevant to phytoplankton dynamics, necessitating studies such as this to determine the role of inflow in the hierarchy of possible influencing factors. This study quantified patterns in nutrients and phytoplankton among three estuaries lying along a naturally occurring freshwater inflow gradient to better understand the role that freshwater inflow plays in phytoplankton dynamics of the region and in similar estuaries elsewhere. It was hypothesized that 1) nutrient concentrations and phytoplankton biomass would be highest in the high inflow estuary (SA) and lower in NC and BB due to lower average inflows, and 2) the phytoplankton community would be distinct among bays and freshwater inflow conditions, dominated by large and/or fast-growing taxa in SA, with the fraction of small and/or slow-growing taxa increasing from NC to BB. As discussed below, results from this study are relevant to these and other estuaries worldwide given changes in freshwater inflow regimes that are being observed.

Over the course of the study, base inflow rates were highest in SA, followed by NC and BB. There were at least seven inflow events to SA where river discharge exceeded 100 $m^3 \cdot s^{-1}$, compared to two in NC and one in BB. These observations are consistent with historical inflow

conditions that exist because of a gradient of decreasing precipitation from the northern estuary (SA) to the southern estuary (BB) (Longley 1994; Montagna et al. 2018). As a result of this inflow gradient as well as high evaporation rates to the south, salinities were lowest on average in SA, intermediate in NC, and highest in BB. NO_x concentrations were significantly different among each of the three bays (SA > BB > NC), with NO_x concentrations ten to fifteen times higher in SA than the other two bays, likely due to both higher average inflows and a watershed that has a high percentage of agricultural land use (Montagna et al. 2018). Property-property plots showed a strong inverse correlation between NO_x and salinity for SA, that was less pronounced in the other two. Ammonium concentrations were typically higher in SA and BB compared to NC. For all three systems, property-property plots showed no correlation between ammonium and salinity, suggestive of internal sources such as regeneration (Morin and Morse 1999; Gardner et al. 2006). BB and SA are also shallower than NC and given the high average wind speed in this region as well as frequency of resuspension events (Carlin et al. 2016; Reisinger et al. 2017; see also: https://windexchange.energy.gov/maps-data/325), injection of ammonium into the water column from sediments is a strong possibility (Lawrence et al. 2004). Overall, the low inorganic nitrogen concentrations observed in NC are consistent with observations of Turner et al. (2015), who also demonstrated low inorganic nitrogen concentrations over the course of a year at several sites in Corpus Christi Bay. Even though the flood conditions observed during late 2018 caused a noticeable drop in salinities of upper NC, there was little to no discernible effect on inorganic nitrogen concentrations in either Nueces or Corpus Christi Bay. This suggests that external nitrogen loads to the system were quickly removed from the water column. Because phytoplankton biomass actually decreased at the Nueces Bay sites during the wet/low salinity period, this leads us to speculate that any riverine

417 inorganic nitrogen loads to NC are rapidly denitrified. Prior work by Gardner et al. (2006)
418 showed that the relative importance of denitrification (a nitrogen removal pathway) compared to
419 DNRA (a nitrogen retention pathway) increased at lower salinities in Texas estuaries. Likewise,
420 Bruesewitz et al. (2013) showed that in nearby Copano Bay, denitrification rates increased
421 following storm events and indicated that the estuary was a net sink for nitrogen during high
422 inflow conditions.

423 Phosphate concentrations were different among all three bays (SA > NC > BB). Property-
424 property plots and regression analysis showed an inverse correlation between phosphate and
425 salinity in each, suggesting that the watersheds are an important source and pointing to the
426 freshwater inflow gradient as a cause of the differences between bays. Furthermore, previous
427 work has shown that BB can be strongly phosphorus-deficient at times, perhaps due to sorption
428 of phosphorus to sediments (Cotner et al. 2004). Silicate concentrations were greater in SA
429 compared to the other two systems, and property-property plots showed an inverse relationship
430 between silicate and salinity for all three bays, supporting a role for freshwater inflow in leading
431 to the higher silicate in SA (see also Paudel et al. 2015). However, silicate concentrations were
432 similar between BB and NC despite differences in inflow. One possibility is that the shallowness
433 of BB promoted enhanced exchange of remineralized silicate from the sediments compared to in
434 the deeper NC, as previous work has suggested that wind-induced resuspension of estuarine
435 sediments can contribute to silicate in the overlying water column (Paudel et al. 2015).

436 The hypothesis that phytoplankton biomass would be highest in SA and decrease along
437 with decreasing inflow from NC to BB was not substantiated. Biovolume was notably higher in
438 BB, in particular during specific high-density events, but lower and roughly equivalent between
439 SA and NC, whereas Chl *a* was high and equivalent in SA and BB, but lower in NC. Secchi

depths were generally shallower in SA, indicating reduced light availability compared to the other two bays. It is well-established that the amount of Chl *a* per cell increases under light-limited conditions (Lewitus et al. 2005; Reynolds 2006). The observed ratio of Chl *a*:biovolume was highest in SA and lowest in BB, supporting the notion that light limitation may have been more pronounced in SA. Light limitation can be a common feature in some estuaries, particularly those such as SA that experience both relatively high freshwater inflow and high turbidity due to mixing (Pennock and Sharp, 1994). Taxon-specific differences in pigment content:biovolume ratio may also play a role. For example, one of the most abundant diatoms observed during bloom periods in BB, *Rhizosolenia*, contains relatively small chloroplasts compared to total cell volume, and in general diatoms often contain a large vacuole, potentially contributing to the lower Chl: biovolume ratios of BB samples compared to SA. More-detailed observations in future studies are needed to fully explain these patterns and discrepancies between Chl *a* and biovolume.

To further explain differences among bays in terms of phytoplankton biomass indicators, we can also look at nutrients. Previous field and experimental studies have shown that N is the main nutrient limiting to phytoplankton growth in many Texas estuaries (Örnólfsdóttir et al. 2004; Dorado et al. 2015), even in BB that occasionally displays very high DIN:DIP ratios (i.e., >16:1; Wetz et al. 2017). As noted above, SA had relatively high inorganic N concentrations throughout the study. Thus, phytoplankton growth in SA would appear less likely to be nutrient limited than in the other two bays, whereas light may be the factor that limits phytoplankton growth potential in it, as previously discussed. Interestingly, despite receiving relatively low inflows on average, BB has undergone eutrophication over the past ~4 decades and has seen long-term increases in both N and Chl *a* concentrations in both the bay and watershed streams

463 (Wetz et al. 2017). This is consistent with work showing that low inflow estuaries such as BB
464 can be particularly susceptible to eutrophication (Bricker et al. 2008; Scavia and Liu 2009).
465 Although it had low inorganic N concentrations, BB had relatively high DON concentrations,
466 some of which is accessible to mixotrophic phytoplankton (Wetz et al. 2017). New work has also
467 indicated the potential for high rates of photoammonification in BB, which would further
468 increase bioavailability of the DON (Liu and Shank 2015, H. Abdulla, unpubl. data). In addition,
469 internal ammonium regeneration rates can be quite high in BB (Morin and Morse 1999; Gardner
470 et al. 2006), providing a continuous N source for phytoplankton. Thus, the eutrophication of BB
471 is the likely cause of its deviation from the expected inflow-phytoplankton relationship, i.e.,
472 phytoplankton biomass is higher than expected from freshwater inflow magnitude alone because
473 of nutrient loading and retention. In contrast, persistent N-limitation is likely in NC, as noted by
474 very low DIN:DIP (mean 2.7 ± 4.6) ratios and the previously discussed low inorganic N
475 concentrations.

476 Despite observing distinct environmental and water chemistry conditions between bays,
477 differences in phytoplankton composition were not pronounced. We hypothesized that larger
478 and/fast growing taxa would be favored in SA, while smaller and/or slower growing taxa would
479 be favored in BB, with a community of intermediate composition in NC. In terms of size
480 fractions, the nanoplankton and microplankton were the overall largest contributor to Chl *a*
481 among all three bays, whereas the contribution of picoplankton was low (<10%) and similar
482 among bays. Thus, the hypothesis was not fully supported. Likewise, diatoms were the dominant
483 phytoplankton group by biovolume in all three bays, consistent with findings from other
484 estuaries worldwide (Carstensen et al. 2015). One common feature of all three estuaries is that
485 they experience high average wind conditions for much of the year (Carlin et al. 2016; Reisinger

et al. 2017; see also: https://windexchange.energy.gov/maps-data/325). Wind-driven turbulence may competitively favor diatoms by maintaining them in the water column, resuspending benthic taxa, and/or by increasing turbidity (Jäger et al. 2008), resulting in reduced light availability and rapidly changing light exposure as cells are transported through the water column – conditions to which many diatoms are specifically well-adapted (Litchman 1998; Depauw et al. 2012). Nonetheless, there were a few noticeable patterns that are worth discussing. First, it appears that the phytoplankton community was generally more diverse in SA than in NC or BB, which we suspect to be due to the influence of freshwater inflow events that act as a disturbance on the phytoplankton community. For example, there were four functional groups that contributed at least 10% of total biovolume in SA on average; diatoms, dinoflagellates, picocyanobacteria and flagellates. In contrast, only diatoms, dinoflagellates and picocyanobacteria contributed at least 10% of total biovolume on average in NC and BB. Furthermore, since 1990, there have been multiple time periods, especially during drought conditions, when prolonged, near monospecific blooms *A. lagunensis* have been observed in BB (Buskey et al. 2001; Cira et al. 2021). As observed here, the communities of both SA and NC tended to see a greater contribution from a larger number of functional groups during inflow events, primarily from flagellates, cyanobacteria and *Mesodinium* in addition to the already numerically significant diatoms and dinoflagellates, adding further evidence for the role of inflow as a disturbance (Buyukates and Roelke 2005). In contrast, the relative contribution of different functional groups of phytoplankton either did not change or decreased in BB during and after inflow events. It is unclear why this was the case, as a previous study showed increased diversity of functional groups during a prolonged wet period in BB (Cira et al. 2021). One possibility is that the inflow events observed during this study were too short in duration to cause noticeable shifts in

community composition, or the preceding dry periods were too short to have established a low diversity community. Another pattern that was observed in both SA and BB was that diatom blooms tended to occur following a lag period after freshwater inflow events, primarily as the inflow was decreasing and presumably flushing was as well. Although additional data is needed to explore this phenomenon in these systems, it is possible that the diatoms may have been outcompeted by e.g., flagellates and dinoflagellates during the ephemeral stratification that occurs immediately following and during freshwater inflow events but are poised to rapidly outcompete those taxa once stratification subsides, taking advantage of the still prevalent nutrients and the diatom's ability to avoid grazing mortality (e.g., Cloern 2005).

Phytoplankton biomass and composition are highly variable in space and time and are influenced by a variety of environmental factors (see e.g., Cloern 2005). Results presented here highlight the importance of freshwater inflow in estuarine phytoplankton dynamics, but also point to other factors (e.g., light availability) that may be important to understand if we are to get a holistic view of phytoplankton community dynamics in estuaries of the study region. In addition, the role of freshwater inflow in shaping estuarine phytoplankton community diversity requires additional attention considering: 1) the general pattern observed here of increased relative importance to overall biovolume from more functional groups in the high inflow SA compared to the other estuaries, 2) the diversification of functional group contributions following inflow events to SA and NC, and 3) the persistence of monospecific harmful blooms of *A. lagunensis* that have been observed in the low inflow BB over the past three decades.

Finally, some conclusions can be reached based on study results in terms of potential impacts of future reductions in freshwater inflow that are expected for the central Texas coast. In the case of NC, long-term decreases in inflow due to damming have already led to increases in

532 salinity and localized decreases in Chl *a* (Kim et al. 2014; Palmer and Montagna 2015; Bugica et
533 al. 2020). Relatively low phytoplankton biovolume and Chl *a* were also observed here. The
534 consequences are unclear, although studies in other systems have shown that this
535 oligotrophication can lead to reductions in upper trophic level production (Nixon et al. 2003). As
536 observed in our study, it appears that riverine N inputs to NC are rapidly removed prior to having
537 an impact on the bay itself. This oligotrophication may be exacerbated if lower inflows continue
538 in the future. However, an alternate future is also possible. Specifically, previous work showing
539 that the relative importance of denitrification compared to DNRA decreases with increasing
540 salinity is relevant (Gardner et al. 2006). This increasing importance of DNRA with increasing
541 salinities would conceivably increase ammonium availability and N retention in the system. This
542 then could lead one to speculate that NC may see less effective denitrification/more effective
543 DNRA in the future under decreasing inflow scenarios, causing it to become more sensitive to
544 external loads. This is important given the rapid urbanization and growing influence of
545 stormwater and wastewater-derived nutrients in the system (Rebich et al. 2011). Further work is
546 needed, given that the negative effects of nutrient retention are already manifesting in the
547 adjacent low inflow estuary, BB. In BB, episodic inflow events appear to stimulate high
548 magnitude blooms, but after a lag period. As noted by a long-term increase in Chl *a* and nutrients
549 (Wetz et al. 2017), the system also appears to be ineffective at removing these nutrients over
550 longer timescales, consistent with emerging evidence of the susceptibility of this and similar low
551 inflow estuaries to the effects of anthropogenic nutrient loadings. Furthermore, dense and/or
552 prolonged blooms of *A. lagunensis* using organic and/or recycled nutrients during lower rainfall
553 conditions cause harm to the ecosystem overall (see e.g., Buskey et al. 2001; Wetz et al. 2017).
554 Drier conditions in the future may lead to more estuaries experiencing similar conditions to BB,

555 with periods of hypersalinity and extended blooms resulting from internal recycling of riverine
556 nutrients received during episodic inflows. The differing responses of each of these ecosystems
557 to freshwater inflow highlight the importance of system-specific management plans and
558 consistent monitoring programs in coastal estuaries.

559

560 ## Acknowledgements

561 We thank Natasha Breaux, Elani Morgan, Josh Martin, Lily Walker, Liz Obst, and Sarah
562 Tominack for assistance in the field, Ken Hayes and Lily Walker for assistance with sample
563 analyses, and Emily Cira and Sarah Tominack for assistance with flow cytometry methods. This
564 research was supported by funding from the Texas Water Development Board (contract
565 no.1800012228), the Celanese Corporation, and an award to TC from the TAMU-CC Division of
566 Research and Innovation's Student Research Competition. This publication was also made
567 possible by the National Oceanic and Atmospheric Administration, Office of Education
568 Educational Partnership Program award (NA16SEC4810009). Its contents are solely the
569 responsibility of the award recipient and do not necessarily represent the official views of the
570 U.S. Department of Commerce, National Oceanic and Atmospheric Administration.

571

572 ## References

573 Agawin, N. S. R., C. M. Duarte, and S. Agustí. 1998. Growth and abundance of *Synechococcus*
574 sp. in a Mediterranean Bay: seasonality and relationship with temperature. Mar. Ecol. Prog.
575 Ser. **170**: 45–53. doi:10.3354/meps170045

576 Álvarez, E., E. Nogueira, and Á. López-Urrutia. 2017. In vivo single-cell fluorescence and size
577 scaling of phytoplankton chlorophyll content. Appl. Environ. Microbiol. **83**:e03317-16.
578 doi:10.1128/AEM.03317-16

579 Azevedo, I. C., A. A. Bordalo, and P. Duarte. 2014. Influence of freshwater inflow variability on
580 the Douro estuary primary productivity: A modelling study. Ecological Modelling **272**: 1–
581 15. doi:10.1016/j.ecolmodel.2013.09.010

582 Bricker, S.B., Longstaff, B., Dennison, W., Jones, A., Boicourt, K., Wicks, C., Woerner, J.,
583 2008. Effects of nutrient enrichment in the nation's estuaries: A decade of change. Harmful
584 Algae 8, 21–32. https://doi.org/10.1016/j.hal.2008.08.028

585 Bruesewitz, D. A., W. S. Gardner, R. F. Mooney, L. Pollard, and E. J. Buskey. 2013. Estuarine
586 ecosystem function response to flood and drought in a shallow, semiarid estuary: Nitrogen
587 cycling and ecosystem metabolism. Limnology and Oceanography **58**: 2293–2309.
588 doi:10.4319/LO.2013.58.6.2293

589 Bugica, K., B. Sterba-Boatwright, and M. S. Wetz. 2020. Water quality trends in Texas estuaries.
590 Mar. Pollut. Bull. **152**: 110903. doi:10.1016/j.marpolbul.2020.110903

591 Buskey, E. J., B. Wysor, and C. Hyatt. 1998. The role of hypersalinity in the persistence of the
592 Texas "brown tide" in the Laguna Madre. J. Plankton Res. **20**: 1553–1565.
593 doi:10.1093/plankt/20.8.1553

594 Buskey, E. J., H. Liu, C. Collumb, and J. G. F. Bersano. 2001. The decline and recovery of a
595 persistent Texas brown tide algal bloom in the Laguna Madre (Texas, USA). Estuaries **24**:
596 337–346.

Buyukates, Y., and D. Roelke. 2005. Influence of pulsed inflows and nutrient loading on zooplankton and phytoplankton community structure and biomass in microcosm experiments using estuarine assemblages. Hydrobiologia **548**: 233-249

Carlin, J. A., G.-H. Lee, T. M. Dellapenna, and P. Laverty. 2016. Sediment resuspension by wind, waves, and currents during meteorological frontal passages in a micro-tidal lagoon. Estuarine, Coastal and Shelf Science **172**: 24–33. doi:10.1016/j.ecss.2016.01.029

Carstensen, J., R. Klais, and J. E. Cloern. 2015. Phytoplankton blooms in estuarine and coastal waters: Seasonal patterns and key species. Estuarine, Coastal and Shelf Science **162**: 98–109. doi:10.1016/j.ecss.2015.05.005

Cira, E. K., T. A. Palmer, and M. S. Wetz. 2021. Phytoplankton dynamics in a low-inflow estuary (Baffin Bay, TX) during drought and high-rainfall conditions associated with an El Niño event. Estuaries and Coasts **44**: 1752–1764. doi:10.1007/s12237-021-00904-7

Cira, E. K., and M. S. Wetz. 2019. Spatial-temporal distribution of *Aureoumbra lagunensis* ("brown tide") in Baffin Bay, Texas. Harmful Algae **89**: 101669. doi:10.1016/j.hal.2019.101669

Cloern, J. E. 2017. Why large cells dominate estuarine phytoplankton. Limnology and Oceanography **63**: S392–S409. doi:10.1002/lno.10749

Collos, Y., B. Bec, C. Jauzein, E. Abadie, T. Laugier, J. Lautier, A. Pastoureaud, P. Souchu, and A. Vaquer. 2009. Oligotrophication and emergence of picocyanobacteria and a toxic dinoflagellate in Thau lagoon, southern France. J. Sea Res. **61**: 68–75. doi:10.1016/j.seares.2008.05.008

618 Cotner, J. B., M. W. Suplee, N. W. Chen, and D. E. Shormann. 2004. Nutrient, sulfur and carbon
619 dynamics in a hypersaline lagoon. Estuarine, Coastal and Shelf Science **59**: 63–652.
620 doi:10.1016/j.ecss.2003.11.008

621 Depauw, F. A., A. Rogato, M. Ribera D'alcalá, and A. Falciatore. 2012. Exploring the molecular
622 basis of responses to light in marine diatoms. Journal of Experimental Botany **63**: 1575–
623 1591. doi:10.1093/jxb/ers005

624 Fahnenstiel, G. L., M. J. McCormick, G. A. Lang, D. G. Redalje, S. E. Lohrenz, M. Markowitz,
625 B. Wagoner, and H. J. Carrick. 1995. Taxon-specific growth and loss rates for dominant
626 phytoplankton populations from the northern Gulf of Mexico. Mar. Ecol. Prog. Ser. **117**:
627 229–239.

628 Felip, M., and J. Catalan. 2000. The relationship between phytoplankton biovolume and
629 chlorophyll in a deep oligotrophic lake: Decoupling in their spatial and temporal maxima.
630 Journal of Plankton Research **22**: 91–105. doi:10.1093/plankt/22.1.91

631 Gardner, W. S., M. J. McCarthy, S. An, D. Sobolev, K. S. Sell, and D. Brock. 2006. Nitrogen
632 fixation and dissimilatory nitrate reduction to ammonium (DNRA) support nitrogen
633 dynamics in Texas estuaries. Limnology and Oceanography **51**: 558–568.
634 doi:10.4319/lo.2006.51.1_part_2.0558

635 Glibert, P. M., J. N. Boyer, C. A. Heil, C. J. Madden, Sturgis B, and Wazniak C S. 2010. Blooms
636 in lagoons: different from those of river-dominated estuaries, *In* Kennish M J and Paerl H
637 W [eds.]. CRC Press.

638 Hart, J. A., E. J. Phlips, S. Badylak, N. Dix, K. Petrinec, A. L. Mathews, W. Green, and A. Srifa.
639 2015. Phytoplankton biomass and composition in a well-flushed, sub-tropical estuary: The

640 contrasting effects of hydrology, nutrient loads and allochthonous influences. Marine
641 Environmental Research **112**: 9–20. doi:10.1016/j.marenvres.2015.08.010

642 Hillebrand, H., C.-D. Durselen, D. Kirschtel, U. Pollingher, and T. Zohary. 1999. Biovolume
643 calculation for pelagic and benthic microalgae. J. Phycol. **35**: 403–424.

644 Jäger, C. G., S. Diehl, and G. M. Schmidt. 2008. Influence of water-column depth and mixing on
645 phytoplankton biomass, community composition, and nutrients. Limnology and
646 Oceanography **53**: 2361–2373. doi:10.4319/LO.2008.53.6.2361

647 Kim, H.-C., S. Son, P. Montagna, B. Spiering, and J. Nam. 2014. Linkage between freshwater
648 inflow and primary productivity in Texas estuaries: Downscaling effects of climate
649 variability. J. Coastal Res. **SI**: 65–73.

650 Kennish, M. J. 2002. Environmental threats and environmental future of estuaries. Conservation
651 **29**: 78–107. doi:10.1017/S0376892902000061

652 Lancelot, C., and K. Muylaert. 2011. Trends in estuarine phytoplankton ecology, p. 5–15. *In*
653 Treatise on estuarine and coastal science. Elsevier Inc.

654 Lawrence, D., M. J. Dagg, H. Liu, S. R. Cummings, P. B. Ortner, and C. Kelble. 2004. Wind
655 events and benthic-pelagic coupling in a shallow subtropical bay in Florida. Marine
656 Ecology Progress Series **266**: 1–13. doi:10.3354/meps266001

657 Lemley, D. A., J. B. Adams, and G. C. Bate. 2016. A review of microalgae as indicators in South
658 African estuaries. S. Afr. J. Bot. **107**: 12–20. doi:10.1016/j.sajb.2016.04.008

659 Lewitus, A. J., D. L. White, R. G. Tymowski, M. E. Geesey, S. N. Hymel, and P. A. Noble.
660 2005. Adapting the CHEMTAX method for assessing phytoplankton taxonomic
661 composition in southeastern U.S. estuaries. Estuaries **28**: 160-172

662 Litaker, R. W., P. A. Tester, C. S. Duke, B. E. Kenney, and J. L. Pinckney. 2002. Seasonal niche
663 strategy of the bloom-forming dinoflagellate *Heterocapsa triquetra*. Ramus Source: Marine
664 Ecology Progress Series **232**: 45–62. doi:10.2307/24865150

665 Litchman, E. 1998. Population and community responses of phytoplankton to fluctuating light.
666 Oecologia **117**: 247–257.

667 Liu, Q., and G. C. Shank. 2015. Solar radiation-enhanced dissolution (photodissolution) of
668 particulate organic matter in Texas estuaries. Estuaries and Coasts **38**: 2172–2184.
669 doi:10.1007/S12237-014-9932-0

670 Longley, W.L.(ed.). 1994. Freshwater inflows to Texas bays and estuaries: ecological
671 relationships and methods for determination of needs. Texas Water Development Board and
672 Texas Parks and Wildlife Department, Austin, TX, 386 pp.

673 Longphuirt, S. N., G. McDermott, S. O'Boyle, R. Wilkes, and D. B. Stengel. 2019. Decoupling
674 abundance and biomass of phytoplankton communities under different environmental
675 controls: A new multi-metric index. Frontiers in Marine Science **6**.
676 doi:10.3389/fmars.2019.00312

677 Mallin, M. A., H. W. Paerl, J. Rudek, and P. W. Bates. 1993. Regulation of estuarine primary
678 production by watershed rainfall and river flow. Marine Ecology Progress Series **93**:
679 199–203. doi:10.3354/meps093199

680 Marie, D., F. Partensky, D. Vaulot, and C. Brussaard. 1999. Enumeration of phytoplankton,
681 bacteria and viruses in marine samples. In: Robinson, J.P, Z. Darzynkiewicz, P.N. Dean, A.
682 Orfao, P.S. Rabinovitch, C.C. Stewart, H.J. Tanke, and L.L. Wheeless (eds), Current
683 protocols in cytometry. 11.11.1-11.11.15

684 McCune, B. and M. J. Mefford. 2018. PC-ORD. Multivariate analysis of ecological data.
685 Version 7.08 Wild Blueberry Media, Corvallis, Oregon, U.S.A.

686 Moisan, T. A., K. L. Blattner, and C. P. Makinen. 2010. Influences of temperature and nutrients
687 on *Synechococcus* abundance and biomass in the southern Mid-Atlantic Bight. Cont. Shelf
688 Res. **30**: 1275–1282. doi:10.1016/j.csr.2010.04.005

689 Montagna, P. A., T. A. Palmer, and J. Beseres Pollack. 2013. Hydrological changes and estuarine
690 dynamics, Springer New York.

691 Montagna, P. A., X. Hu, T. A. Palmer, and M. Wetz. 2018. Effect of hydrological variability on
692 the biogeochemistry of estuaries across a regional climatic gradient. Limnology and
693 Oceanography **63**: 2465–2478. doi:10.1002/lno.10953

694 Morin, J., and J. W. Morse. 1999. Ammonium release from resuspended sediments in the Laguna
695 Madre estuary. Marine Chemistry **65**: 97–110.

696 Murrell, M. C., R. S. Stanley, E. M. Lores, G. T. DiDonato, and D. A. Flemer. 2002. Linkage
697 between microzooplankton grazing and phytoplankton growth in a Gulf of Mexico estuary.
698 Estuaries **25**: 19–29. doi:10.1007/BF02696046

699 Nielsen-Gammon, J. W., J. L. Banner, B. I. Cook, and 9 others. 2020. Unprecedented drought
700 challenges for Texas water resources in a changing climate: what do researchers and
701 stakeholders need to know? Earth's Future **8:** doi:10.1029/2020EF001552

702 Nixon, S. W. 2003. Replacing the Nile: Are anthropogenic nutrients providing the fertility once
703 brought to the Mediterranean by a great river? Ambio **32**: 30–39.

704 Örnólfsdóttir, E. B., S. E. Lumsden, and J. L. Pinckney. 2004. Nutrient pulsing as a regulator of
705 phytoplankton abundance and community composition in Galveston Bay, Texas. Journal of
706 Experimental Marine Biology and Ecology **303**: 197–220. doi:10.1016/j.jembe.2003.11.016

707 Paerl, H. W., N. S. Hall, B. L. Peierls, K. L. Rossignol, and A. R. Joyner. 2014. Hydrologic
708 variability and its control of phytoplankton community structure and function in two
709 shallow, coastal, lagoonal ecosystems: the Neuse and New River estuaries, North Carolina,
710 USA. Estuaries and Coasts **37**: 31–45. doi:10.1007/s12237-013-9686-0

711 Paerl, H. W., L. M. Valdes-Weaver, A. R. Joyner, and V. Winkelmann. 2007. Phytoplankton
712 indicators of ecological change in the eutrophying Pamlico Sound System, North Carolina.
713 Ecological Applications **17**: S88–S101. doi:10.1890/05-0840.1

714 Palmer, T. A., and P. A. Montagna. 2015. Impacts of droughts and low flows on estuarine water
715 quality and benthic fauna. Hydrobiologia **753**: 111–129. doi:10.1007/s10750-015-2200-x

716 Paudel, B., P.A. Montagna, and L. Adams. 2015. Variations in the release of silicate and
717 orthophosphate along a salinity gradient: do sediment composition and physical forcing
718 have roles? Estuarine, Coastal and Shelf Science **157**: 42-50

719 Pennock, J.R., Sharp, J.H., 1994. Temporal alternation between light-limitation and nutrient-
720 limitation of phytoplankton production in a coastal plain estuary. Mar. Ecol. Prog. Ser. 111,
721 275–288. https://doi.org/10.3354/meps111275

722 Phlips, E. J., S. Badylak, and T. C. Lynch. 1999. Blooms of the picoplanktonic cyanobacterium
723 *Synechococcus* in Florida Bay, a subtropical inner-shelf lagoon. Limnol. Oceanogr. **44**:
724 1166–1175. doi:10.4319/lo.1999.44.4.1166

725 R Core Team. 2020. R: A language and environment for statistical computing.Rebich, R. A., N.
726 A. Houston, S. V. Mize, D. K. Pearson, P. B. Ging, and C. E. Hornig. 2011. Sources and
727 delivery of nutrients to the Northwestern Gulf of Mexico from streams in the South-Central
728 United States. J. Am. Water Resour. Assoc. **47:** 1061–1086. doi:10.1111/j.1752-
729 1688.2011.00583.x

730 Reisinger, A., J. C. Gibeaut, and P. E. Tissot. 2017. Estuarine suspended sediment dynamics:
731 observations derived from over a decade of satellite data. Frontiers in Marine Science 4:
732 https://doi.org/10.3389/fmars.2017.00233

733 Reynolds, C. S. 2006. The ecology of phytoplankton, Cambridge University Press.

734 Robinson, D., and A. Hayes. 2020. broom: Convert Statistical Analysis Objects into Tidy
735 Tibbles.

736 Roelke, D. L., H. P. Li, N. J. Hayden, C. J. Miller, S. E. Davis, A. Quigg, and Y. Buyukates.
737 2013. Co-occurring and opposing freshwater inflow effects on phytoplankton biomass,
738 productivity and community composition of Galveston Bay, USA. Marine Ecology Progress
739 Series **477**: 61–76. doi:10.3354/meps10182

740 Rose, J. M., and D. A. Caron. 2007. Does low temperature constrain the growth rates of
741 heterotrophic protists? Evidence and implications for algal blooms in cold waters. Limnol.
742 Oceanogr. **52**: 886–895.

743 Pennock, J.R., Sharp, J.H., 1994. Temporal alternation between light-limitation and nutrient-
744 limitation of phytoplankton production in a coastal plain estuary. Mar. Ecol. Prog. Ser. 111,
745 275–288. https://doi.org/10.3354/meps111275

746 Scavia, D., Liu, Y., 2009. Exploring estuarine nutrient susceptibility. Environ. Sci. Technol. 43,
747 3474–3479. https://doi.org/10.1021/es803401y

748 Sklar, F. H., and J. A. Browder. 1998. Coastal environmental impacts brought about by
749 alterations to freshwater flow in the Gulf of Mexico. Environ. Management **22**: 547-562

750 Strom, S. L., E. L. Macri, and M. B. Olson. 2007. Microzooplankton grazing in the coastal Gulf
751 of Alaska: Variations in top-down control of phytoplankton. Limnol. Oceanogr. **52**: 1480–
752 1494. doi:10.4319/lo.2007.52.4.1480

753 Sullivan, J. M., and E. Swift. 2003. Effects of small-scale turbulence on net growth rate and size
754 of ten species of marine dinoflagellates. J. Phycol **39**: 83–94.

755 Sun, J., and D. Liu. 2003. Geometric models for calculating cell biovolume and surface area for
756 phytoplankton. J. Plankton Res. **25**: 1331–1346. doi:10.1093/plankt/fbg096

757 Texas Water Development Board. 2019. Bays & Estuaries.

758 Turner, E. L., B. Paudel, and P. A. Montagna. 2015. Baseline nutrient dynamics in shallow well
759 mixed coastal lagoon with seasonal harmful algal blooms and hypoxia formation. Mar.
760 Pollut. Bull. **96**: 456–462. doi:10.1016/j.marpolbul.2015.05.005

761 Underwood, G., and J. Kromkamp. 1999. Primary production by phytoplankton and
762 microphytobenthos in estuaries. Adv. Ecol. Res. **29**: 93–153. doi:10.1016/S0065-
763 2504(08)60192-0

764 USEPA. 1999. Ecological condition of estuaries in the Gulf of Mexico. EPA 620-R-98-004. EPA
765 620-R-98-004 U.S. Environmental Protection Agency, Office of Research and
766 Development, National Health and Environmental Effects Research Laboratory.

767 Waring, E., M. Quinn, McNamara Amelia;, E. A. de la Rubia, Zhu Hao;, and S. Ellis. 2021.
768 skimr: Compact and Flexible Summaries of Data. R Version 2.1.3.

769 Welschmeyer, N.A. 1994. Fluorometric analysis of chlorophyll a in the presence of chlorophyll b
770 and phaeopigments. Limnology and Oceanography **39:** 1985-1992

771 Wetz, M. S., E. K. Cira, B. Sterba-Boatwright, P. A. Montagna, T. A. Palmer, and K. C. Hayes.
772 2017. Exceptionally high organic nitrogen concentrations in a semi-arid South Texas
773 estuary susceptible to brown tide blooms. Estuarine, Coastal and Shelf Science **188**: 27–37.
774 doi:10.1016/j.ecss.2017.02.001

775 Wetz, M. S., E. A. Hutchinson, R. S. Lunetta, H. W. Paerl, and J. C. Taylor. 2011. Severe
776 droughts reduce estuarine primary productivity with cascading effects on higher trophic
777 levels. Limnology and Oceanography **56**: 627–638. doi:10.4319/lo.2011.56.2.0627

778 Wickham, H., M. Averick, J. Bryan, and others. 2019. Welcome to the Tidyverse. Journal of
779 Open Source Software **4**: 1686. doi:10.21105/joss.01686

780 Yacobi, Y. Z., and T. Zohary. 2010. Carbon:chlorophyll a ratio, assimilation numbers and
781 turnover times of Lake Kinneret phytoplankton. Hydrobiologia **639**: 185–196.
782 doi:10.1007/s10750-009-0023-3

783

784

785